EJNMMI Research

SHORT COMMUNICATION Open Access

Quantification of [^{11}C]PBR28 data after systemic lipopolysaccharide challenge

Eric A. Woodcock[1], Martin Schain[2], Kelly P. Cosgrove[3] and Ansel T. Hillmer[3*]

Abstract

Background: Lipopolysaccharide (LPS) is a classic immune stimulus. LPS combined with positron emission tomography (PET) 18 kDa translocator protein (TSPO) brain imaging provides a robust human laboratory model to study neuroimmune signaling. To evaluate optimal analysis of these data, this work compared the sensitivity of six quantification approaches.

Methods: [^{11}C]PBR28 data from healthy volunteers (N = 8) were collected before and 3 h after LPS challenge (1.0 ng/kg IV). Quantification approaches included total volume of distribution estimated with two tissue, and two tissue plus irreversible uptake in whole blood, compartment models (2TCM and 2TCM-1k, respectively) and multilinear analysis-1 (MA-1); binding potential estimated with simultaneous estimation (SIME); standardized uptake values (SUV); and SUV ratio (SUVR).

Results: The 2TCM, 2TCM-1k, MA-1, and SIME approaches each yielded substantive effect sizes for LPS effects (partial η^2 = 0.56–0.89, ps <. 05), whereas SUV and SUVR did not.

Conclusion: These findings highlight the importance of incorporating AIF measurements to quantify LPS-TSPO studies.

Keywords: [^{11}C]PBR28 PET imaging, TSPO, Neuroimmune, Neuroinflammation, Lipopolysaccharide

Introduction

Positron emission tomography (PET) imaging of the 18 kDa translocator protein (TSPO) provides a quantitative measure of an in vivo neuroimmune system marker [1]. While interpretation of baseline TSPO levels is complicated by several factors [2], TSPO response after lipopolysaccharide (LPS) challenge yields a measurement of "neuroimmune response" to an acute immunogenic stimulus. LPS is gram-negative bacteria that evokes classic pro-inflammatory responses via the toll-like receptor-4 complex (TLR4). Preclinical PET studies indicate intra-striatal LPS injection increases TSPO levels relative to contralateral striatal levels and saline-injected controls; findings confirmed by autoradiography and cold-tracer studies [3, 4]. Prior research demonstrates LPS increases brain TSPO levels across species, including rodents [3, 4], nonhuman primates [5], and humans [6]. Thus, LPS challenge provides a robust experimental model for investigating neuroimmune signaling in people.

The dramatic LPS effects on specific binding motivate reanalysis and confirmation of quantification approaches. In most cases, reference region approaches are not appropriate for full quantification of TSPO radioligands due to the lack of regions devoid of TSPO in the brain, although pseudo-reference region approaches have been validated for specific scenarios [7]. In this study, we evaluated the sensitivity of different TSPO quantification approaches to LPS effects, with careful consideration of approaches incorporating an arterial input function, using previously reported data with the second-generation PET TSPO radiotracer [^{11}C]PBR28 [6]. Specifically, we evaluated analytic approaches which incorporate an arterial input function (AIF): total volume of distribution (V_T) estimated with a two-tissue compartment model (2TCM), a 2TCM variant which includes a parameter purported to describe irreversible uptake in endothelial cells (2TCM-1k) [8], multilinear analysis-1 (MA-1) [9], and estimation of binding potential (BP_P) with simultaneous estimation (SIME) [10]. We

* Correspondence: ansel.hillmer@yale.edu
[3]Department of Radiology & Biomedical Imaging, Yale School of Medicine, 330 Cedar St., New Haven, CT, USA
Full list of author information is available at the end of the article

also evaluated semi-quantitative metrics that do not incorporate an AIF: standardized uptake values (SUV) and SUV ratio (SUVR). We hypothesized that models that incorporate the AIF (2TCM, 2TCM-1k, MA-1, and SIME) would be more sensitive to LPS-induced TSPO increases.

Methods

Recruitment

The Yale University School of Medicine Human Investigation Committee and the Radioactive Drug Research Committee approved all study procedures. Subjects were genotyped for the rs6971 polymorphism: only "high-" and "mixed-affinity binders" were eligible (HABs and MABs, respectively). Subjects (N = 8; 5 MABs, 24.9 ± 5.5 years old, 87.5 ± 12.3 kg, 8 M) were recruited, screened, and enrolled as previously described [6]. All subjects provided written informed consent.

Experimental procedures

All subjects participated in one experimental session consisting of two 120-minute [^{11}C]PBR28 PET scans on the same day. Following the baseline [^{11}C]PBR28 PET scan, subjects were injected with LPS (1.0 ng/kg IV), NIH Clinical Center Reference Endotoxin *E. coli* serotype O:113. The second [^{11}C]PBR28 PET scan started 3 h after the LPS injection.

Data processing

PET acquisition details have been fully described elsewhere [11]. Briefly, [^{11}C]PBR28 was synthesized with high molar activity 569 ± 327 MBq/nmol (15.4 ± 8.8 mCi/nmol). [^{11}C]PBR28 was injected via slow bolus (1 min), and PET data were acquired for 120 min on the high resolution research tomograph (HRRT, Siemens) with simultaneous optical head motion tracking (Vicra, NDI Systems). Dynamic list-mode data were histogrammed into intervals ranging from 30 s to 5 min and reconstructed using the MOLAR algorithm. T_1-weighted structural MR images were coregistered to PET data for region of interest (ROI)-based extraction of time-activity curves (TACs) determined in AAL template space. ROIs assessed included the caudate, cerebellum, hippocampus, thalamus, putamen, and frontal, parietal, temporal, and occipital cortices. Arterial blood samples were collected throughout each 120-minute scan to measure the metabolite-corrected AIF and plasma free fraction (f_p), as previously described [6, 12].

Analytic approaches

Area under the curve (AUC) of the metabolite-corrected AIF was calculated using numerical trapezoidal integration. Imaging data were analyzed using each approach: 1TCM, 2TCM, 2TCM-1k, MA-1, SIME, SUV, and SUVR. Plasma uptake delay (τ) was estimated using a 1TCM from the first 10 min of data and was fixed for 2TCM and 2TCM-1k analyses. Compartment modeling analyses were performed with the Compartment Model Kinetic Analysis Tool (COMKAT [13]) in the MATLAB environment. 1TCM poorly described ROI TACs; therefore, results are not reported. In the 2TCM model, four rate constants were estimated: K_1, k_2, k_3, and k_4 [14]. The 2TCM-1k model includes a fifth parameter (k_b) that models purported irreversible uptake in endothelial cells [8]. The corrected Akaike Information Criterion (AICc [15]) indicated model preference for a fixed blood volume fraction (V_b = 5%) for 2TCM and 2TCM-1k. For MA-1 [9], V_T was estimated using t^* = 30, consistent with prior work [11]. Simultaneous estimation (SIME) simultaneously fits TACs across all ROIs to estimate whole-brain V_{ND} which, in combination with regional V_T values, can estimate ROI binding potentials specific to total plasma concentration (BP_P) [10]. Due to the low free fraction (~ 2%) resulting in poor f_P precision [16], analyses incorporating f_p in V_T estimates are only included for completeness as Additional file 1. Finally, SUV was calculated as mean tissue activity concentration for each ROI during specified timeframes (60–90 min, 90–120 min) normalized by subject body weight and injected [^{11}C]PBR28 dose. SUVR was estimated by dividing ROI SUV by whole-brain SUV. AICc was used to compare model parsimony for 2TCM vs. 2TCM-1k [15].

Repeated measures analyses of variance (rmANOVA) were used to evaluate LPS effects on each calculated endpoint (statistical transformations applied as needed to normalize distributions) across ROIs (within-subject factor) with rs6971 genotype (HAB vs. MAB) as a between-subject factor (significance threshold: $p < .05$). Partial eta-squared (η^2) effect sizes were estimated from rmANOVAs.

Results

The AIF AUC significantly decreased after LPS across rs6971 genotypes (F (1, 6) = 41.06, partial η^2 = 0.87; Fig. 2a; group average time curves shown in Additional file 1: Figure S1). In the brain, 2TCM V_T and 2TCM-1k V_T (inverse-transformed) significantly increased after LPS by 47% and 24% on average, respectively (2TCM: F (1, 6) = 38.39, partial η^2 = 0.87; 2TCM-1k: F (1, 6) = 7.55, partial η^2 = 0.56; Table 1; Figs. 1 and 2). Mean AICc values indicated 2TCM was preferred to 2TCM-1k (2TCM, 20.0 ± 0.49 and 20.3 ± 0.78; 2TCM-1k, 23.5 ± 0.75 and 23.89 ± 1.38; pre- and post-LPS, respectively). MA-1 V_T and SIME BP_P significantly increased after LPS by 45% and 82% on average, respectively (F (1, 6) = 39.02, partial η^2 = 0.87, and F (1, 6) = 49.29, partial η^2 = 0.89, respectively). Importantly, whole-brain SIME V_{ND} did not significantly change from pre- to post-LPS (p = .39). SIME

Table 1 LPS effects

Model	Parameter	LPS Effect				
		Partial η^2	95% CI	Overall (%)	MABs (%)	HABs (%)
AIF AUC	AUC	0.87**	0.47–0.92	− 32.6	− 30.0	− 38.1
2TCM	V_T	0.87**	0.45–0.92	46.7	56.4	38.9
2TCM-1k	V_T	0.56*	0.03–0.74	24.3	10.4	34.6
MA-1	V_T	0.87**	0.46–0.92	44.9	53.3	37.8
SIME	BP_P	0.89**	0.53–0.93	81.9	94.1	61.5
SUV, 60–90 min	SUV	0.35	0.00–0.61	− 9.9	− 1.4	− 19.8
SUV, 90–120 min	SUV	0.07	0.00–0.39	− 1.5	8.7	− 13.6
SUVR, 60–90 min	SUVR	0.34	0.00–0.61	− 3.0	− 1.4	− 5.5
SUVR, 90–120 min	SUVR	0.15	0.00–0.46	− 1.3	− 0.7	− 4.3

LPS effect % = [(Post-LPS − Pre-LPS)/Pre-LPS] × 100. Partial η^2 effect size interpretation: "Small" ≤ 0.09, "Moderate" = 0.10–0.24, "Large" ≥ 0.25. *95% CI* 95% confidence interval for the partial η^2 effect size at $p = .05$. Significant LPS effects are noted

*$p \leq .05$

**$p < .01$

BP_P, 2TCM V_T, and MA-1 V_T exhibited the largest LPS effects (partial η^2 = 0.87–0.89; Table 1; Fig. 1; Additional file 1: Figure S2). SUV and SUVR estimated smaller LPS effects (partial $\eta^2 \leq 0.35$), which indicated an apparent decrease in TSPO levels from baseline.

Discussion

This work indicates that peripheral LPS administration significantly reduced the [^{11}C]PBR28 AIF AUC by 33%. Approaches that incorporate the AIF (2TCM V_T, 2TCM-1k V_T, MA-1 V_T, and SIME BP_P) yielded large effect sizes for TSPO increases following LPS administration. The SIME, 2TCM, and MA-1 approaches yielded nearly identical sensitivity (partial η^2 = 0.87–0.89), while 2TCM-1k was less sensitive, albeit still yielding a large effect size (partial η^2 = 0.56). AICc values preferred 2TCM to 2TCM-1k. SIME estimates of BP_P are directly proportional to TSPO levels (i.e., do not include nondisplaceable uptake) and therefore provide theoretically improved estimates of specific binding. BP_P yielded the largest percentage increase following LPS challenge (82%), but also greater variability and thus a nearly identical effect size as 2TCM V_T and MA-1 V_T. Notably, V_{ND} estimated with SIME did not change pre- to post-LPS. Estimation of V_T/f_p also yielded significant LPS-induced increases (Additional file 1) but smaller effect sizes than V_T due to the variability in f_p estimation. No evidence for LPS effects on f_p measurements was found. Therefore, we conclude that 2TCM, MA-1,

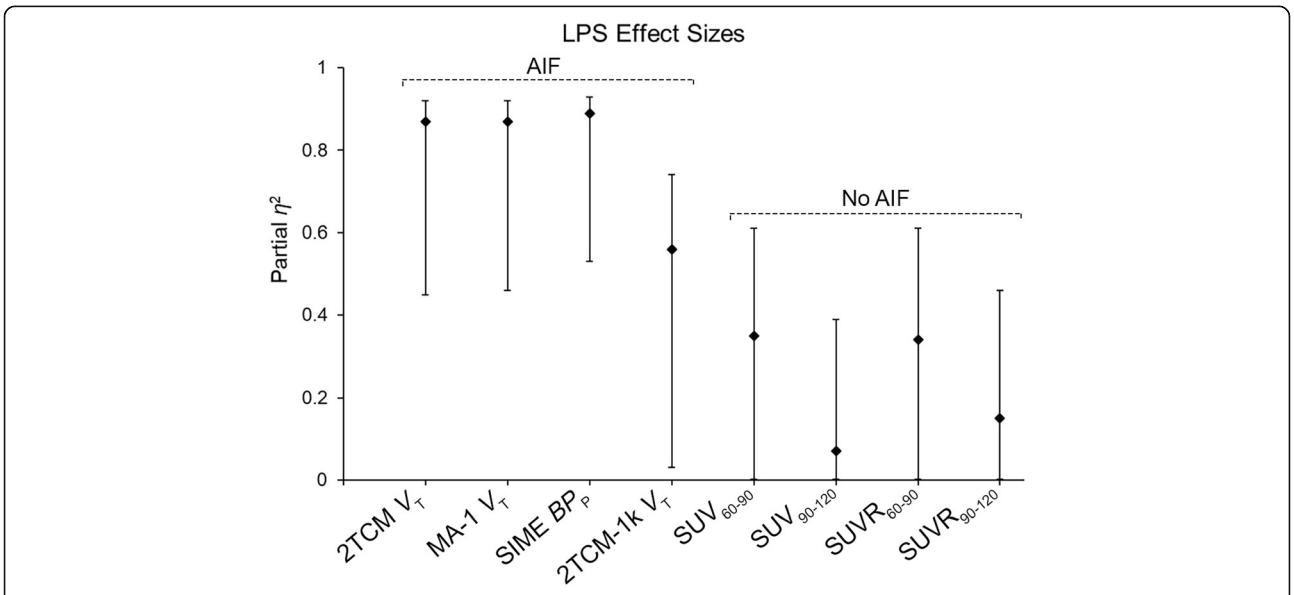

Fig. 1 LPS effect sizes (partial η^2) and 95% confidence intervals for each analytic approach are depicted

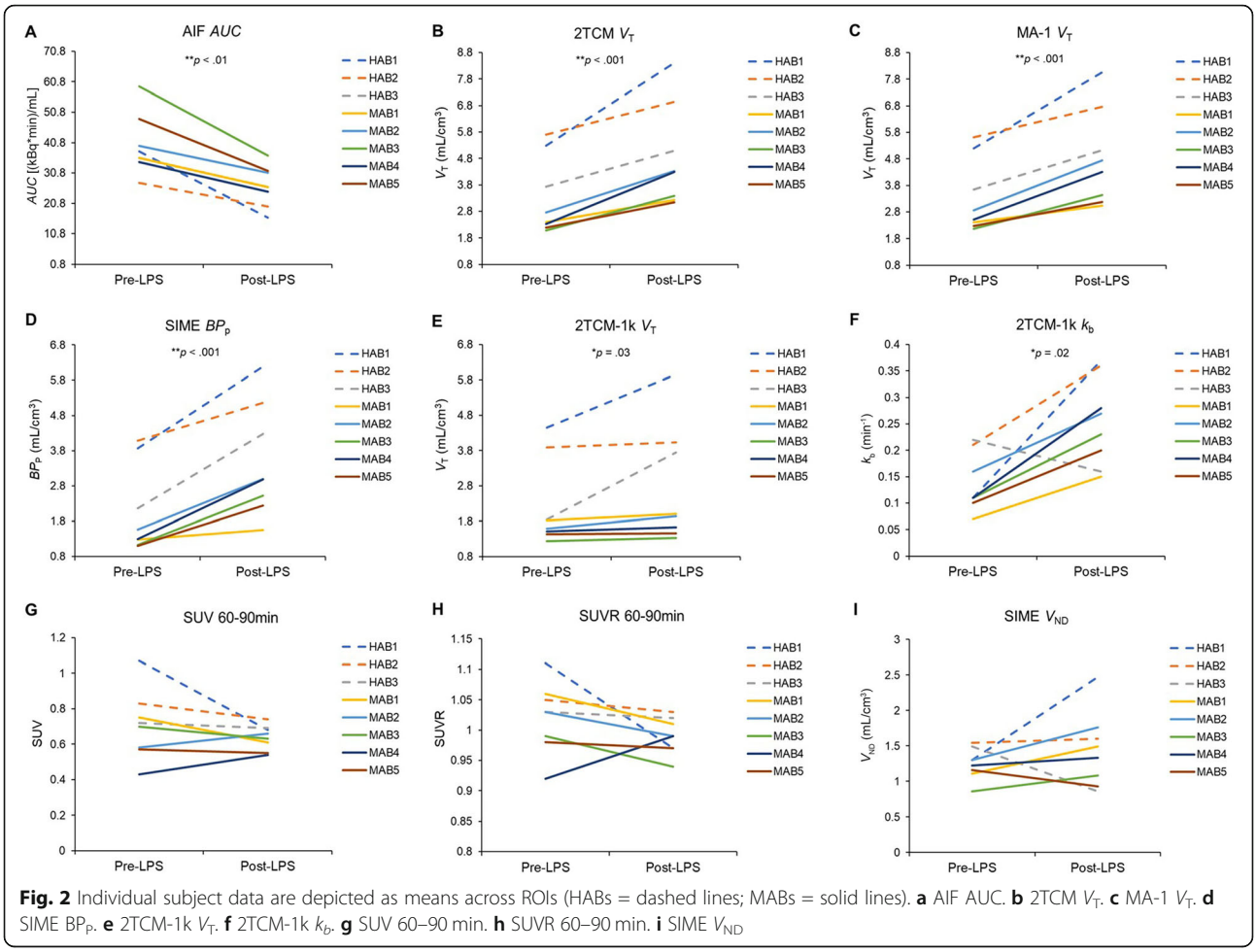

Fig. 2 Individual subject data are depicted as means across ROIs (HABs = dashed lines; MABs = solid lines). **a** AIF AUC. **b** 2TCM V_T. **c** MA-1 V_T. **d** SIME BP_P. **e** 2TCM-1k V_T. **f** 2TCM-1k k_b. **g** SUV 60–90 min. **h** SUVR 60–90 min. **i** SIME V_{ND}

and SIME are the most sensitive quantitative approaches to estimate TSPO availability in the context of this LPS paradigm.

In contrast, semi-quantitative approaches that do not incorporate AIF measurements (SUV and SUVR) failed to detect significant LPS-induced TSPO increases in the brain. The significant reduction in AIF AUC suggests increased [^{11}C]PBR28 specific binding in the periphery and may explain the poor performance of SUV in this context. The global [^{11}C]PBR28 V_T increase after LPS confirms the lack of suitable reference region for TSPO in this context and contributed to the poor performance of SUVR. Taken together, these findings highlight the importance of the metabolite-corrected AIF for LPS challenge studies, and support previous cautionary conclusions in the use of SUV-based quantification of TSPO [17, 18].

LPS is a classic immune stimulus shown to evoke robust neuroimmune responses. Preclinical findings indicate LPS increased brain TSPO levels which were co-localized with activated microglia (CD11b and OX2 immunoreactivity) and astrocytes (GFAP immunoreactivity), increased expression of toll-like receptors (TLR-2 and TLR-4), and increased brain cytokine levels [3, 4, 19]. LPS administration substantially increases TSPO immunohistochemical markers, mRNA levels, and protein expression in rodents [20, 21]. PET imaging studies confirm that LPS upregulates TSPO levels across species [3–5], including humans [6]. In sum, this literature strongly supports our expectation that brain TSPO should increase in response to systemic LPS administration.

Limitations of this work include our inability to confirm whether LPS activates microglia and/or astrocytes and recruits additional TSPO-expressing cells, or any combination of these or other properties [22]. Additionally, future research is needed to investigate if less invasive approaches, i.e., venous input functions, can replace the AIF.

In conclusion, our findings indicate that analytic approaches that incorporate the AIF are necessary to detect LPS effects on brain TSPO levels. The findings highlight the importance of the metabolite-corrected AIF for quantification of LPS-induced [^{11}C]PBR28 brain changes.

Supplementary information

Supplementary information accompanies this paper at https://doi.org/10.1186/s13550-020-0605-7.

Additional file 1: Supplemental Material. **Table S1. Figure S1.** Mean AIF data are depicted separately for rs6971 genotype HABs (C/C; gray lines) and MABs (C/T; black lines) pre-LPS (solid lines) and post-LPS (dashed lines). **Figure S2.** Individual values, pre- and post-LPS, are depicted for each brain region for models that incorporate the AIF: A) 2TCM VT; B) 2TCM-1k VT; C) MA-1 VT (t*=30); and D) SIME BPP. The same color marker was used to depict each subject's data across models and LPS dose (pre- vs. post-LPS). **Figure S3.** A Time-Activity Curve was extracted from the occipital cortex (OCC) of a representative subject and kinetic model fit are depicted: A) pre-LPS 2TCM; B) post-LPS 2TCM; C) pre-LPS 2TCM-1k; and D) post-LPS 2TCM-1k.

Abbreviations

2TCM: Two-tissue compartment model; AICc: Akaike information criterion corrected; AIF: Arterial input function; AUC: Area under the curve; BP: Binding potential; f_p: Plasma free fraction; HRRT: High resolution research tomograph; LPS: Lipopolysaccharide; MA-1: Multilinear analysis-1; PET: Positron emission tomography; ROI: Region of interest; SIME: Simultaneous estimation; SUV: Standardized uptake value; SUVR: Standardize uptake value ratio; TACs: Time-activity curves; TLR2: Toll-like receptor-2; TLR4: Toll-like receptor-4 complex; TSPO: 18 kDa translocator protein; V_T: Total volume of distribution

Acknowledgements

The authors thank the Yale PET center staff.

Authors' contributions

KPC designed the study and supervised the data collection. EAW, MS, and ATH analyzed the data. EAW and ATH drafted the initial manuscript. All authors have read and approved the final manuscript.

Funding

Funding generously provided by the NIH: K99 DA048125 (EAW), T32 DA022975 (postdoctoral fellow: EAW), K01 AA024788 (ATH), R01 MH110674 (KPC), and the VA National Center for PTSD (KPC). MS was supported by the NARSAD Young Investigator Grant.

Availability of data and materials

Due to the sensitive nature of human participant information, data are available upon reasonable request by contacting the corresponding author.

Ethics approval and consent to participate

The Yale University School of Medicine Human Investigation Committee approved this study (HIC #1305011987), and all the subjects provided informed consent prior to participation.

Consent for publication

Not applicable.

Competing interests

The authors declare that they have no competing interests.

Author details

[1]Department of Pscyhiatry, Yale School of Medicine, 300 George St., New Haven, CT, USA. [2]Neurobiology Research Unit, Copenhagen University Hospital, Copenhagen, Denmark. [3]Department of Radiology & Biomedical Imaging, Yale School of Medicine, 330 Cedar St., New Haven, CT, USA.

Received: 13 December 2019 Accepted: 31 January 2020
Published online: 12 March 2020

References

1. Rupprecht R, Papadopoulos V, Rammes G, Baghai TC, Fan J, Akula N, et al. Translocator protein (18 kDa)(TSPO) as a therapeutic target for neurological and psychiatric disorders. Nature reviews Drug discovery. 2010;9:971–88.
2. Notter T, Coughlin J, Sawa A, Meyer U. Reconceptualization of translocator protein as a biomarker of neuroinflammation in psychiatry. Mol Psychiatry. 2018;23:36.
3. Dickens AM, Vainio S, Marjamaki P, Johansson J, Lehtiniemi P, Rokka J, et al. Detection of microglial activation in an acute model of neuroinflammation using PET and radiotracers 11C-(R)-PK11195 and 18F-GE-180. J Nucl Med. 2014;55:466–72.
4. Sridharan S, Lepelletier F-X, Trigg W, Banister S, Reekie T, Kassiou M, et al. Comparative evaluation of three TSPO PET radiotracers in a LPS-induced model of mild neuroinflammation in rats. Molecular Imaging and Biology. 2017;19:77–89.
5. Hannestad J, Gallezot J-D, Schafbauer T, Lim K, Kloczynski T, Morris ED, et al. Endotoxin-induced systemic inflammation activates microglia: [11 C] PBR28 positron emission tomography in nonhuman primates. Neuroimage. 2012; 63:232–9.
6. Sandiego CM, Gallezot J-D, Pittman B, Nabulsi N, Lim K, Lin S-F, et al. Imaging robust microglial activation after lipopolysaccharide administration in humans with PET. Proc Natl Acad Sci. 2015;112:12468–73.
7. Lyoo CH, Ikawa M, Liow J-S, Zoghbi SS, Morse CL, Pike VW, et al. Cerebellum can serve as a pseudo-reference region in Alzheimer disease to detect neuroinflammation measured with PET radioligand binding to translocator protein. J Nuclear Med. 2015;56:701–6.
8. Rizzo G, Veronese M, Tonietto M, Zanotti-Fregonara P, Turkheimer FE, Bertoldo A. Kinetic modeling without accounting for the vascular component impairs the quantification of [11C] PBR28 brain PET data. J Cerebral Blood Flow Metabol. 2014;34:1060–9.
9. Ichise M, Toyama H, Innis RB, Carson RE. Strategies to improve neuroreceptor parameter estimation by linear regression analysis. J Cerebral Blood Flow Metabol. 2002;22:1271–81.
10. Ogden RT, Zanderigo F, Parsey RV. Estimation of in vivo nonspecific binding in positron emission tomography studies without requiring a reference region. NeuroImage. 2015;108:234–42.
11. Hillmer A, Sandiego C, Hannestad J, Angarita G, Kumar A, McGovern E, et al. In vivo imaging of translocator protein, a marker of activated microglia, in alcohol dependence. Mol Psychiatry. 2017.
12. Hannestad J, DellaGioia N, Gallezot J-D, Lim K, Nabulsi N, Esterlis I, et al. The neuroinflammation marker translocator protein is not elevated in individuals with mild-to-moderate depression: a [11 C] PBR28 PET study. Brain, Behav Immuni. 2013;33:131–8.
13. Muzic RF Jr, Cornelius S. COMKAT: compartment model kinetic analysis tool. J Nuclear Med. 2001;42:636–45.
14. Innis RB, Cunningham VJ, Delforge J, Fujita M, Gjedde A, Gunn RN, et al. Consensus nomenclature for in vivo imaging of reversibly binding radioligands. J Cerebral Blood Flow Metabol. 2007;27:1533–9.
15. Hurvich CM, Tsai C-L. Regression and time series model selection in small samples. Biometrika. 1989;76:297–307.
16. Park E, Gallezot J-D, Delgadillo A, Liu S, Planeta B, Lin S-F, et al. 11 C-PBR28 imaging in multiple sclerosis patients and healthy controls: test-retest reproducibility and focal visualization of active white matter areas. European journal of nuclear medicine and molecular imaging. 2015;42:1081–92.
17. Matheson GJ, Plavén-Sigray P, Forsberg A, Varrone A, Farde L, Cervenka S. Assessment of simplified ratio-based approaches for quantification of PET [11C]PBR28 data. EJNMMI Res. 2017;7:58. https://doi.org/10.1186/s13550-017-0304-1.
18. Yoder KK, Territo PR, Hutchins GD, Hannestad J, Morris ED, Gallezot J-D, et al. Comparison of standardized uptake values with volume of distribution for quantitation of [11C] PBR28 brain uptake. Nuclear Med Biol. 2015;42:305–8.
19. Hoogland ICM, Houbolt C, van Westerloo DJ, van Gool WA, van de Beek D. Systemic inflammation and microglial activation: systematic review of animal experiments. J Neuroinflammation. 2015;12:114. https://doi.org/10.1186/s12974-015-0332-6.
20. Karlstetter M, Nothdurfter C, Aslanidis A, Moeller K, Horn F, Scholz R, et al. Translocator protein (18 kDa) (TSPO) is expressed in reactive retinal microglia and modulates microglial inflammation and phagocytosis. J Neuroinflammation. 2014;11:3. https://doi.org/10.1186/1742-2094-11-3.
21. Bae K-R, Shim H-J, Balu D, Kim SR, Yu S-W. Translocator protein 18 kDa negatively regulates inflammation in microglia. J Neuroimmune Pharmacol. 2014;9:424–37.

22. Owen DR, Narayan N, Wells L, Healy L, Smyth E, Rabiner EA, et al. Pro-inflammatory activation of primary microglia and macrophages increases 18 kDa translocator protein expression in rodents but not humans. J Cerebral Blood Flow Metabol. 2017;37:2679–90.

Publisher's Note